Eurographics Workshop on Visual Computing for Biology and Medicine (2016)
S. Bruckner, B. Preim, and A. Vilanova (Editors)

A framework for fast initial exploration of PC-MRI cardiac flow

A.J.M. Broos[1], N.H.L.C. de Hoon[2], P.J.H. de Koning[3], R.J. van der Geest[3], A. Vilanova[2] and A.C. Jalba[1]

[1]Computer Science and Mathematics, Eindhoven University of Technology, The Netherlands
[2]Electrical Engineering, Mathematics and Computer Science, Delft University of Technology, The Netherlands
[3]Department of Radiology, Leiden University Medical Center, The Netherlands

Abstract

Cardiac flow is still not fully understood, and is currently an active research topic. Using phase-contrast magnetic resonance imaging (PC-MRI) blood flow can be measured. For the inspection of such flow, researchers often rely on methods that require additional scans produced by different imaging modalities to provide context. This requires labor-intensive registration and often manual segmentation before any exploration of the data is performed. This work provides a framework that allows for a quick exploration of cardiac flow without the need of additional imaging and time-consuming segmentation. To achieve this, only the 4D data from one PC-MRI scan is used. A context visualization is derived automatically from the data, and provides context for the flow. Instead of relying on segmentation to deliver an accurate context, the heart's ventricles are approximated by half-ellipsoids that can be placed with minimal user interaction. Furthermore, seeding positions for flow visualization can be placed automatically in areas of interest defined by the user and based on derived flow features. The framework enables a user to do a fast initial exploration of cardiac flow, as is demonstrated by a use case and a user study involving cardiac blood flow researchers.

Categories and Subject Descriptors (according to ACM CCS): I.3.8 [Computer Graphics]: Applications—4D PC-MRI Blood-Flow I.4.9 [Computer Graphics]: Picture/Image Generation—Image Processing and Computer Vision I.3.3 [Computer Graphics]: Picture/Image Generation—Line and Curve Generation

1. Introduction

Cardiovascular diseases (CVDs) have the highest world-wide mortality rates [Mea15]. It is known that changes in anatomy have influence on the blood flow and, furthermore, haemodynamics affects the cardiovascular anatomy [HBB*10, MFK*12]. The blood flow of an individual, therefore, is an important factor in gaining insight in both the occurrence and progression of CVDs. However, blood flow within the heart is still not fully understood, and remains a large research topic. Modern imaging techniques, such as Doppler ultra-sound and phase contrast magnetic resonance imaging (PC-MRI), can be used to acquire the velocity of the blood flow. Of these techniques, 4D PC-MRI provides the most complete volumetric velocity data over time. For the inspection of the flow, being able to select areas of interest is important to avoid occlusion and clutter. Furthermore, certain flow patterns, such as vortices, are of great interest to researchers of cardiac blood flow [EvdGC*16]. However, without a targeted selection of interesting areas to explore, targeted placement of seed points for the flow visualization, vortices or other flow phenomena are occluded and can be easily overlooked. To this end a 2D slice of the 3D morphology is often shown to provide context for the flow visualization given by the measurements. While 3D context visualizations for blood flow exist, they are mainly focused on vessels. These vessels do not change their shape much, and flow within them often has a clear general direction. The heart on the other hand, has a more dynamic shape over time, furthermore, the flow is highly turbulent. Therefore, a segmentation of the heart provides anatomical context, and allows visualization of the flow from and to a segments also enabling quantitative inspection. Creating such a segmentation, however, is often done manually and is a tedious and time-consuming process. While some insight might be gained into the morphology of the heart by using the signal magnitude or the temporal magnitude intensity projection of the PC-MRI measurements, other types of imaging techniques can provide a much higher resolution and contrast. However, registration is needed to align the data, since the scans are made at different points in time and possibly by different scanners. Furthermore, for a fast and initial exploration of the data, an initial visualization that does not require tedious segmentation would be beneficial.

This work investigates the possibilities for exploration of 4D cardiac flow PC-MRI data without resorting to time-consuming preprocessing or manual labor. A framework is presented providing an interaction and visualization strategy to obtain a complete visualization of the cardiac blood flow based on a single 4D PC-MRI data set. The data consists of time-resolved magnitude and three di-

DOI: 10.2312/vcbm.20161273

rectional velocity data. More details on the acquisition of PC-MRI and its applications are given by Markl et al. [MFK*12].

In summary, the contributions of this paper are:

- Investigation and proposal of context visualization without the need of additional imaging or tedious segmentation.
- An intuitive interactive selection of the areas of interest.
- A feature-based seeding for cardiac flow visualization.
- A user study to evaluate the different aspects of the framework

2. Related work

Multiple frameworks for the exploration of PC-MRI data exist [KBvP*16]. However, these focus mainly on the exploration of vascular flow instead of flow in the heart. Our work can be divided in the following parts: context visualization, ventricle approximation and selection of areas of interest based on features are used.

2.1. Context visualization

Anatomical context visualization provides the user an anatomical reference for the flow visualization. Many different approaches for such a visualization exist. The dataset can be shown on the background or a plane in a 3D visualization [GZM97, SAG*14]. Another approach is to extract surfaces from the data and render those for anatomical context visualization [GNBP11, vPBB*10]. These surfaces can come from manual segmentation, automatic segmentation [SV97, CNC*10], or user-guided automatic segmentation [YPH*06]. For these segmentations to work well, much higher quality anatomical data compared to the available magnitude obtained from the PC-MRI data must be used. Kohlmann et al. [KBKG07] made a framework that automatically creates a volume rendered view, based on what the user marked as areas of interest on a 2D slice. Illustrative techniques can be used to emphasize the focus of your visualization, and abstract from unnecessary details [BCP*12]. Using few colors in the shading of the context visualization can make it less distracting while still providing enough perception of its structure [vPBB*10]. Contour lines can be used to emphasize this structure even more [KWTM03]. Bruckner et al. [BG07] created transfer functions that interpolate between different illustrative styles, called lit sphere maps [SMGG01], instead of colors. Clipping of the volume rendering is usually done using planes or boxes, but other voxelized clipping volumes have been used as well [WEE02] making it a viable candidate for our goal.

2.2. Ventricle approximation

The ventricles are often an area of interest when inspecting cardiac flow. While many different methods for automatic segmentation of the ventricles exist [HGL*14, LGW06, CNN*08], all of them require higher quality anatomical data to be available. Pelt et al. [vPBB*11] developed a virtual probe that can be placed manually or fitted to a vessel, defining a volume of interest where we want to inspect flow. This probe is intended for vessels and the fitting requires laminar flow. The probe's shape is a truncated cone, which fits the tubular structure of vessels well. For the left ventricle however, a half-ellipsoid shape provides a better approximation [KNC*05].

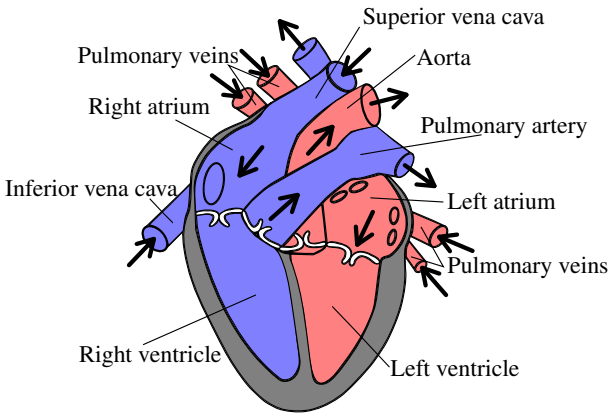

Figure 1: Anatomy of the human heart. Red indicates oxygenated blood, while blue indicates oxygen-poor blood. The arrows show the flow direction.

2.3. Feature-based flow visualization

Features can be derived from the flow, which can provide more information or indicate interesting flow patterns. One flow pattern that has received much attention in cardiac flow is the vortex. Different approaches to identify them exist, partly due to the existence of many different definitions of a vortex [JH95, Hal05, vPFCV14]. Research has gone into the tracking of features over time as well. Features arise, change and fade over time in unsteady flow fields. These moments of creation and destruction, as well as the area encompassed by the feature at each timestep in between, can be visualized on a timeline [PVH*03, MM09]. Both Stalling et al. [SZH97] and Doleisch et al. [DGH03] worked on visualization based on features. Their approaches are based on a feature definition provided by the user to define their own features, these features can then be used to define seeding areas for the flow visualization. Whereas we support the combination of 1D features, they allow for higher dimensional data, at the price of a more complex system. Our framework allows the user to guide the seeding process based on features.

3. Medical background

In this section, a brief summary on the anatomy of the heart is given. Figure 1 schematically shows the anatomy of the human heart and the general flow directions. The heart is separated into a left and a right side by a muscle called the septum. At the top there are two atria, and at the bottom, the ventricles are located. When the atria contract, the blood inside is pushed through the valves and fills up the ventricles. Here, the tricuspid and mitral valves serve as one-way doors: blood should not flow back in when the right and left ventricle respectively when they contract. Then, when the ventricles contract, blood is pushed through the pulmonary valve into the lungs and through the aortic valve into the rest of the body. These valves serve as one-way doors as well.

Arteries have blood flowing away from the heart, while veins have blood flowing towards the heart. When no distinction is made, veins and arteries are usually called blood vessels. The pulmonary

artery leads oxygen-poor blood to the lungs, whereas the pulmonary veins lead oxygen-rich blood from the lungs back into the heart. The aorta is an artery that leads oxygen-rich blood to the body, while the inferior and superior vena cava lead oxygen-poor blood back into the heart.

An efficient blood flow is essential, since the main task of the heart is to provide oxygenated blood to the rest of the body. For example, the blood can, in case of a so-called mitral valve regurgitation, flow back from the left ventricle into the left atrium. This leakage can increase blood volume and pressure in the left atrium and the pulmonary veins. In severe cases, the heart can be enlarged to provide flow of blood in the aorta, potentially causing heart failure. Furthermore, the increased pressure in the left atrium and the pulmonary veins can result in congestion (or fluid build-up) in the lungs.

4. Context visualization

In this Section, we introduce the anatomical context visualization. The aim is to provide insight into the anatomical relation of the flow, without being too distracting. Two options are available for the basis of the context visualization: the so-called t-MIP or the magnitude data (PCA-M) of the PC-MRI measurement. The temporal maximum intensity projection of the flow speed (t-MIP) contains for each voxel the maximum speed it reaches over time.

Existing straightforward 3D visualizations, such as surface or volume rendering do not work well when using the magnitude data of the PC-MRI measurement as a basis for anatomical context due to the challenging data, as shown in Figure 2 left. Note that both the resolution and contrast are low, resulting in less then ideal visualization of the anatomy.

Often, slices of anatomical data are used as context for flow visualization. However, the heart is not two-dimensional. It takes experience and time to comprehend how such a slice corresponds to the three-dimensional anatomical data.

Another approach is to define an iso-surface based on the t-MIP, it can then be used to render an iso-surface using, for example, marching cubes [vPBB*10]. Using clipping techniques, for example only showing the back faces, or drawing the flow on top of the rendering, this approach can provide a good context when inspecting vessels. However, by using the t-MIP the anatomy changes over time are lost, which for the dynamic morphology of the heart is less suitable compared to the more static vessels. Furthermore, the flow speed is relatively low in the ventricles and atria, resulting in low contrast for the t-MIP dataset.

Illustrative techniques provide means to emphasize shape and take the focus away from unnecessary details. In this work, volume rendering is taken as a base and several techniques are implemented to improve the anatomical context visualization. Slice visualizations such as multiplanar reformat (MPR) and view-orthogonal plane visualizations are available to provide a higher level of detail.

Our goal is to obtain a s much high quality context as possible given the PC-MRI data.

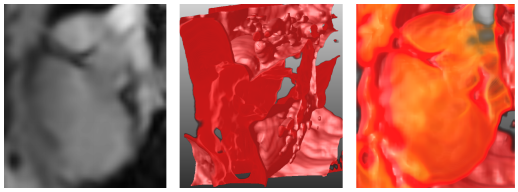

Figure 2: Context visualizations using the magnitude data of the PC-MRI measurement. From left to right: a single slice, an iso-surface and a volume rendering.

4.1. Illustrative transparency

The context visualization should not occlude the flow visualization, therefore, the volume rendering should not be fully opaque. When uniformly decreasing the opacity of the context visualization, it can become hard to perceive the morphology. Instead, illustrative transparency [BG07] is implemented as it emphases the contours, making the rest of the context more transparent. Contours are view-dependent, that is, they represent the edges of structures from our point of view. See Figure 3 for an example of illustrative transparency, note that for illustration purposes we are using the t-MIP and therefore just the main vessels are visible.

The illustrative transparency is computed for a given scalar field I. The gradient vector field $\vec{G} = \nabla I$ is calculated, allowing us to look up the gradient $\vec{g}$ for a position within the field. We define a surface to be on the contour when it faces a direction somewhat perpendicular to our view direction $\vec{v}$. The direction a sample faces, i.e. the normal of a sample, is determined by the gradient $\vec{g}$ at that point: $\vec{n} = \vec{g}/||\vec{g}||$. Then, the contour variable c is defined as

$$c = \max(0, \vec{n} \cdot \vec{v} - k), \tag{1}$$

where k is a limit for the angle between $\vec{n}$ and $\vec{v}$, based on the curvature at the sample point. When $c = 0$ for a sample, that sample is on the contour, otherwise c has a positive value.

Contours are regulated based on the normal curvature along the view direction [KWTM03, BG07]. The normal curvature along the view direction was approximated by taking the angle between the normals of two subsequent sampling points along a sampling ray. Along the sampling ray $\vec{v}$, two points p_0 and p_1 are sampled subsequently that have normals $\vec{n}_0$ and $\vec{n}_1$. The angle α between those normals is used to approximate the curvature at p_1. We can now define the limit k as done by Kindlmann et al. [KWTM03] from Equation 1 using:

$$a = \frac{\cos(\alpha)}{s}, \tag{2}$$

$$k = \sqrt{w \cdot a \cdot (2 - w \cdot a)}, \tag{3}$$

where a is the approximation of the normal curvature, with s being the distance between p_0 and p_1. Then, k is the limit for contours defined by Bruckner et al. [BG07], where w is a parameter to control the width of the contours.

As described earlier, normals are given by the gradient of input data I. But in homogeneous regions, neighboring gradients can have very strong variations in direction, while their magnitudes are

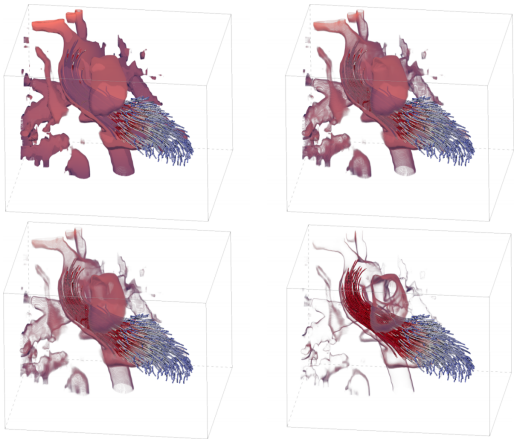

Figure 3: Flow from the left ventricle into aorta during systole. Context visualization using the t-MIP dataset with illustrative transparency increasing from top-left to bottom-right.

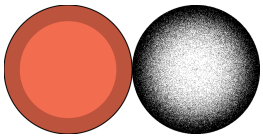

Figure 4: Examples of lit sphere maps (LSM). The pink LSM (left) was drawn by hand and the dotted one (right) was generated.

all very low. To combat the effect of the varying normals in homogeneous regions on c, a measure h for homogeneity is defined as:

$$h = 1 - \frac{||\vec{g}||}{||g_{max}||} \tag{4}$$

where g_{max} is the highest magnitude gradient found in the dataset.

Now, the transparency at a sample point p_s is defined such that it has a higher value for samples further away from the contour, i.e.,

$$p_s = p_{tf}^{0.5+ch}, \tag{5}$$

where p_{tf} is the sample's transparency value determined by the transfer function. The constant exponent of 0.5 was determined empirically [BG07]. Now by increasing the transparency in the transfer function for our context visualization, we can emphasize contours and therefore the morphology's structure, as shown in Figure 3. Note that only vessels can be visualized, moreover, the low resolution and contrast of the magnitude data makes it less usable there.

4.2. Lit sphere maps

Lit sphere maps (LSM) [SMGG01] are textures that define a lighting and coloring style on a sphere, as shown in Figure 4. Providing an easy and effective way to generate illustrative renderings. The normal of every sample is projected onto a plane orthogonal to the view direction. When placing the center of the LSM at the base of the normal vector, the end of the vector projects onto a pixel in the LSM. This pixel determines the color of the sample. This enables different illustrative styles for the context visualization. In Figure 5, different LSMs are applied. Due to their abstract nature, the LSMs provide a context visualization without distracting the user from the flow.

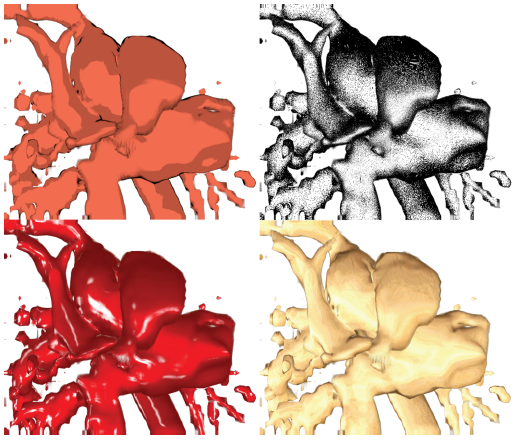

Figure 5: Context rendered with different lit sphere maps (LSM). Top row, from left to right: flat pink, dotted, bottom row, from left to right: muscle and bone. The muscle and bone-like LSMs are based on Bruckner et al. [BG07].

We propose to generate a dotted lit sphere map as follows. A uniform distributed random sample $u \in [0, 2\pi]$ is taken. Another sample w is taken from an exponential distribution with probability density function $f(a) = \lambda e^{\lambda a}$, where $a \in [0, \infty)$. We then calculate positions of black pixels $(x, y) \in [-1, 1] \times [-1, 1]$ such that the angle is uniformly distributed and the radius exponentially:

$$r = 1 - w \tag{6}$$

$$x = r \cdot \cos(u) \tag{7}$$

$$y = r \cdot \sin(u) \tag{8}$$

Note that if w exceeds 1, another sample is drawn. This process is repeated N times, with N being the number of pixels in the image. Using the above technique ensures more black pixels will be at the border of the disk, resulting in an emphasis of the contour. For the dotted image in Figures 4 and 5 the image size is 512×512 and $\lambda = 8$.

4.3. Depth enhancement

The above illustrative volume rendering techniques do not encode the depth, making it difficult to discern spatial relations. For this purpose, two techniques were implemented, depth-based tone manipulation and depth-based transparency manipulation.

Depth-based tone manipulation uses color to give samples at the start of the ray a warmer color, while giving samples at the end of the ray a cooler color. The depth cue comes from the perception that cool colors recede while warm colors advance [GGSC98, LM02]. Here, a tone from yellow (warm) to blue (cool) is used to map from near to far, respectively.

Depth-based transparency changes transparency based on depth. We found that the transparency at a sample point p_t defined by

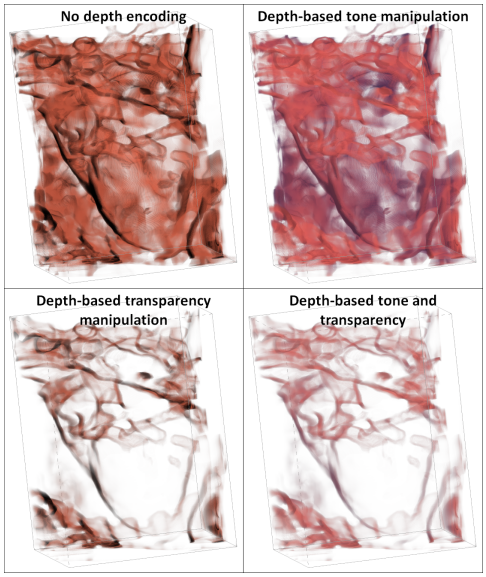

Figure 6: Comparison of context visualization using different depth-based manipulations.

$p_t = p_{tf} \cdot \sqrt{d}$ works well. Here, $d \in [0,1]$ is the depth, and p_{tf} is the sample's transparency value determined by the transfer function.

Combining both depth encodings does not bring much improvement since the transparency manipulation reduces the effect of the cooler colors in the back. Figure 6 shows the two methods used in combination with a a volume rendering of the heart. We have generated several context visualizations based on t-MIP or PC-MRI magnitude data to investigate the use of this information as context. In Section 7 an evaluation is made to see whether and how these context visualizations can be used.

5. Ventricle approximation

Seed points are often needed for flow visualization techniques, e.g., pathlines and particles. Placing such points manually is tedious and time-consuming. Therefore, seeding regions are commonly defined wherein seed points are automatically generated.

A key observation by Kovalova et al. [KNC*05] is that the ventricles can be approximated by half ellipsoids; i.e., the left ventricle has a shape similar to half of an ellipsoid, while the right ventricle is wrapped around it, as seen in Figure 7. Here, LVE stands for the set of voxels inside the left ventricle ellipsoid and RVE stands for the set of voxels inside right ventricle ellipsoid. The ventricles will be modeled by ellipsoids without any account for wall thickness. Here, the set of voxels inside the right ventricle is defined by $RVE \setminus LVE$. Notice that for the purpose of seeding and visualization an approximation of the location should in general be sufficient.

Tri-axial ellipsoids can be placed by the user; an overview is shown in Figure 8, where the center point is denoted by c, its orthonormal axes are $\vec{v}_1$, $\vec{v}_2$ and $\vec{v}_3$, and the radii along those axes are given by λ_1, λ_2 and λ_3, respectively. The half ellipsoid can be defined by the user using three guide points. For the placement of

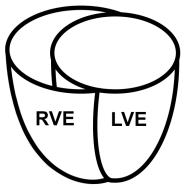

Figure 7: Geometric approximation of the ventricles using ellipsoids: the left ventricle ellipsoid (LVE) and the right ventricle ellipsoid (RVE). The right ventricle is approximated by $RVE \setminus LVE$.

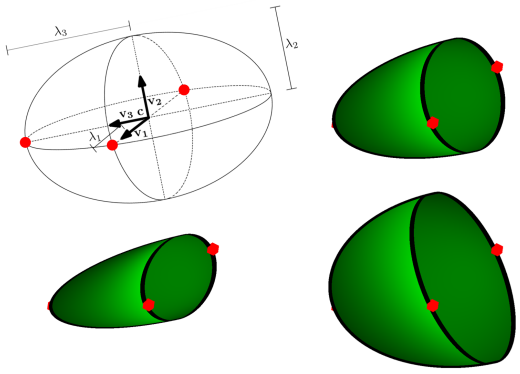

Figure 8: A tri-axial ellipsoid with center point c. The orthonormal axes are given by $\vec{v}_1$, $\vec{v}_2$ and $\vec{v}_3$. The radii along those axes are λ_1, λ_2 and λ_3. Initially $\lambda_2 = \lambda_1$ (top right). The user can vary λ_2 to squeeze (lower left) or stretch the ellipsoid (lower right).

these points the user can inspect the magnitude and t-MIP using the multiplanar reformat visualization or the view-orthogonal plane visualization. The user places the guiding points g_1, g_2 and g_3 on these planes which then define a half ellipsoid. One point represents the apex and the other two points should be near the atrium of the corresponding ventricle.

The center point c is derived as $c = (g_1 + g_2)/2$. Furthermore, $\vec{v}_2$ is defined as the vector pointing towards the view and $\vec{v}_3 = c - g_3$. $\vec{v}_1$ is expected to be orthogonal to the other vectors, hence it is computed as $\vec{v}_1 = \vec{v}_3 \times \vec{v}_2$. Since $\vec{v}_1$ is orthogonal to $\vec{v}_3$, it is possible that the half-ellipsoid does not line up with the first two guiding points. Therefore, a clipping plane is used that passes through those two points. λ_1, λ_2 and λ_3 can be derived from the distance between the center and guide points. Since λ_2 is not defined by the guide points it will initially be set to λ_1, however, the user can easily vary this value to squeeze or stretch the ellipsoid. This allows users to the define half ellipsoids to estimate the ventricles with little user interaction.

The seed points can now be generated within LVE and $RVE \setminus LVE$ to investigate the flow in both ventricles. To avoid occlusion, only the contours of the ellipsoids are rendered throughout this paper.

6. Feature-based flow visualization

When inspecting cardiac flow, researchers are often interested in certain flow features, such as speed or vorticity. Our feature-based seeding approach aims to facilitate quick identification of such areas, and automatic placement of seed points similar to Stalling et al [SZH97].

Using transfer functions the user can directly influence the seeding probability of the location where a value of the selected flow feature occurs. That is, for every voxel v, the value v_f for a certain feature f can be calculated. Based on that value, a seeding probability $p_{v_f} \in [0,1]$ is determined by the transfer function. Multiple transfer functions can also be combined.

The following features are provided:

- Flow speed magnitude
- Magnitude data (PCA-M)
- Curl
- λ_2-criterion
- Q-criterion

Measures of vorticity are often used to inspect cardiac flow. Such rotation of flow can be computed using the curl, which describes the rotation of a 3-dimensional vector field. The curl of a vector field is a vector field itself. Every vector represents the axis of rotation, according to the right-hand rule, and the magnitude of the curl vector represents the amount of rotation.

To compute the curl we compute the gradient tensor of the vector field F at position $\vec{x}$:

$$G(\vec{x}) = \begin{bmatrix} \frac{\partial F_x}{\partial x} & \frac{\partial F_x}{\partial y} & \frac{\partial F_x}{\partial z} \\ \frac{\partial F_y}{\partial x} & \frac{\partial F_y}{\partial y} & \frac{\partial F_y}{\partial z} \\ \frac{\partial F_z}{\partial x} & \frac{\partial F_z}{\partial y} & \frac{\partial F_z}{\partial z} \end{bmatrix} \tag{9}$$

From this, the curl at position $\vec{x}$ is given by:

$$\vec{curl}(\vec{x}) = \begin{bmatrix} \frac{\partial F_z}{\partial y} - \frac{\partial F_y}{\partial z} \\ \frac{\partial F_x}{\partial z} - \frac{\partial F_z}{\partial x} \\ \frac{\partial F_y}{\partial x} - \frac{\partial F_x}{\partial y} \end{bmatrix} \tag{10}$$

Often, the core of the vortex, the region around which the vortex rotates, is of interest. Such areas are often found using both the so-called λ_2-criterion and the Q-criterion. For the computation of the λ_2-criterion the rate-of-strain tensor S and vorticity tensor Ω are computed:

$$S(\vec{x}) = \frac{G(\vec{x}) + G^T(\vec{x})}{2} \tag{11}$$

$$\Omega(\vec{x}) = \frac{G(\vec{x}) - G^T(\vec{x})}{2} \tag{12}$$

From these, the three eigenvalues $\lambda_1 \geq \lambda_2 \geq \lambda_3$ of $S(\vec{x})^2 + \Omega(\vec{x})^2$ are computed. If two eigenvalues are negative for a given point, that is $\lambda_2 < 0$, it lays in a vortex core. Similarly, for the Q-criterion if the value of Q is positive the point is part of a vortex core, where Q is given by

$$Q(\vec{x}) = \frac{||S(\vec{x})||^2 - ||\Omega(\vec{x})||^2}{2} \tag{13}$$

The user can use a transfer function to define the probability of a seed being placed in a voxel based on its value for the selected feature. An example of feature-based seeding is shown in Figure 9. Here the region shown in magenta depicts the area where $\lambda_2 < -30$. This region is used to distribute seed points for pathlines. A combination of features can be used by defining multiple transfer functions for multiple features. The probabilities are in this case multiplied to obtain the seeding probability per voxel.

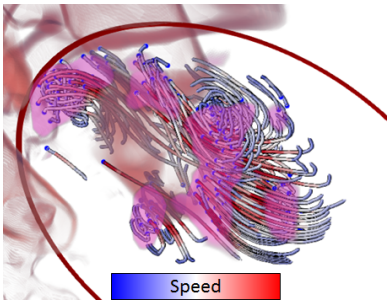

Figure 9: Pathlines seeded (blue points) using the λ_2-criterion, showing several vortices inside the left ventricle during early diastole. The area shown using magenta is the seeding region, where $\lambda_2 < -30$.

7. Evaluation

In this section our application is evaluated using a use case and a user study held among 6 4D PC-MRI flow researchers.

For the evaluation, two datasets were used: a healthy volunteer and patient data. For the healthy volunteer 30 phases were measured covering a single heartbeat, yielding a temporal resolution of 32ms. Providing $65 \times 55 \times 25$ voxels with a size of $2.27 \times 2.27 \times 4.20$mm. The patient data covered a full heart cycle in 30 phases with a temporal resolution of 40ms. Resulting in 30 volumes with $70 \times 55 \times 38$ voxels each sized $2.27 \times 2.27 \times 3.00$mm.

7.1. Use case

For this use case, the context visualization is used to obtain a reference with the vessels. The context visualization, however, does not clearly show the ventricles themselves, as shown in Figure 10a. Therefore, a slice depicting the speed is aligned with the vessels, shown in Figure 10b. The selected slice is of a phase during systole, so the aorta shows in bright white; this eases the search for the left ventricle (denoted by LV). The view-orthogonal plane is used to place the slice approximately through the middle of the LV. Guide points are placed on the slice to create the left ventricle ellipsoid (LVE) in Figure 10c. The opacity on the context visualization has been decreased, to allow us to see flow within the vessels, while the contours are still emphasized. After hiding the slice, the flow is inspected further. During early systole, we notice that not all the blood seems to flow into the aorta. Some of the flow seems to go back into the direction of the left atrium, as shown in Figure 10d. To further investigate, another ellipsoid is placed. By tracing the pathlines backwards through time from the left ventricle, the left atrium can be found at a phase in diastole, see Figure 10e. The second ellipsoid can now be placed on the slice. Using forward tracing

pathlines, the flow into left ventricle can be seen in Figure 10f suggesting correct placement of the ellipsoid. Since the position of the unexpected flow in Figure 10d and Figure 10f match, this indicates the need for further inspection of the so-called mitral valve. This finding was confirmed by the researchers at (LUMC). This is further supported by Figure 10h which shows flow behind the mitral valve back into the left atrium, while in a healthy volunteer, shown in Figure 10g, the blood behind the mitral valve remains relatively still. If not all blood flows towards the aorta during systole, but it flows in the left atrium this indicates a dysfunction of the mitral valve.

7.2. User study

The goal of this work is to enable initial cardiac flow exploration without time-consuming manual preprocessing. To see whether the visualization generated would fulfill the exploratory needs, 4D flow experts were questioned. Six researchers from the cardiology and radiology departments of the LUMC filled out a questionnaire. Before the questionnaire, they were given an overview of the project by means of a small presentation. Then, a demonstration per single component of the tool was shown, after which the experts filled in the questionnaire for that specific component. The project was divided into context visualization, ventricle ellipsoids, and feature-based seeding components. Finally, they were asked for their general opinions and suggestions. The questionnaire can be found in the additional materials. In this section, the results of the questionnaire are presented. A Likert-scale was used in the questions that were formulated as a statement and the researchers could tick a box depending on their agreement with the statement. The results of the questionnaire are shown Table 1. Here, + indicates that many of them agreed, +/- indicates that opinions differed, while - indicates that they disagreed with the statement.

Questions involving choices between options presented in figures and open questions will be discussed separately.

7.3. Context visualization

Two options were available for the basis of the context visualization: the t-MIP or the PCA-M datasets. There was a unanimous preference for the t-MIP data as a basis. All the researchers agreed that the general structure of the heart could be perceived from the context, whereas all except one agreed that it helps with understanding the flow. The ventricles and atria were not visible in the context visualization, however, all agreed that the slices provide this additional information. Especially the view-orthogonal plane was much appreciated.

While depth-based transparency manipulation helps with the PCA-M based context visualization, depth-based color manipulation was preferred for depth perception by all researchers. Several options for the lit sphere maps were presented, with the favorite being the flat pink LSM with four votes, shown top left in Figure 5. The remaining two votes went to the bone-like LSM, also shown in Figure 5 (bottom right). When asked if they would use the context visualization, 4 said yes. One was not sure, and the remaining expert thought it was not applicable to their work.

7.4. Ventricle approximation

All researchers agreed that in general the ventricles could be well approximated using the ventricle ellipsoids. However, for rare patients with, for example, a single ventricle defect it might not provide a good approximation. Placing three guiding points on a slice seemed intuitive to the researchers. They also agreed that a clipping ellipsoid can be a better fit for the shape of a heart, compared to planes or boxes. When asked if they would use the ventricle ellipsoids, all agreed that they would use it. Even for the less appropriate cases; some patients have severely different morphology for the ventricles, they might still work well for defining the region of interest.

7.5. Feature-based flow visualization

All 6 researches agreed that areas of interest could be defined using flow features and seed points could be placed within them automatically. While most agreed that transfer functions were an intuitive way to specify properties of these areas of interest, two were neutral on this part. Clinical use was mentioned, however, would be limited since doctors would not be familiar with transfer functions. Opinions were divided when asked whether they would use feature-based seeding. While areas of interest could be specified, some would not want to automatically fill the whole areas, but rather use it as a guide for manual placement of seed points. Opinions also differed about the need for more than two features being combined. Other features that were suggested to be interesting are ones related to wall-shear stress, velocity direction compared to a given vector, and helical flow.

7.6. General feedback

The goal of this work was to enable exploration of cardiac flow for a quick initial overview. It was unanimously agreed that this goal was achieved. 5 experts thought there was a need for such software, the remaining expert was not sure. However, two researchers noted that the research side generally is not interested in new ways of qualitative inspection anymore. Both mentioned that the framework would be very suitable for clinical, on-site use. Suggestions for future work included improving the user interface for clinical use, more flow visualization options compared to just pathlines and particles, trying the software on many different heart diseases, and interpolating the ventricle ellipsoids over time between two placements: one for systole and one for diastole.

8. Conclusion and future work

The aim of this paper was to provide a framework that aids a fast exploration of cardiac flow. For this purpose, anatomical context visualization for flow was explored. While direct volume rendering of the magnitude data was initially to be the basis of the context visualization, this data was found to be unsuitable as a context in most situations. The temporal maximum intensity projection, t-MIP, led to a better visualization of the context. It provides a good initial point of orientation, and provides a clear context for flow in the main vessels around the heart, which also aids in identifying the general location of the heart. Applying illustrative transparency the

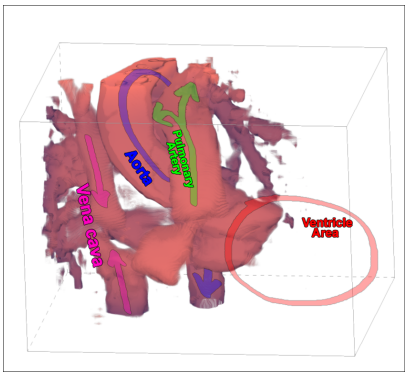

(a) Our context visualization showing the vessels. Here magenta shows the vena cava, blue the aorta, green the pulmonary artery and red indicates the expected location of the ventricles.

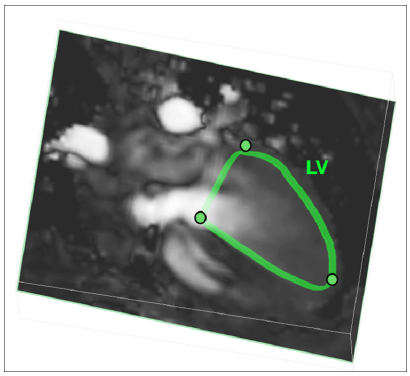

(b) A slice at systole through the vessels. On the slice white means high flow speed while black represents low speeds. The green outline denotes an approximation of the Left Ventricle.

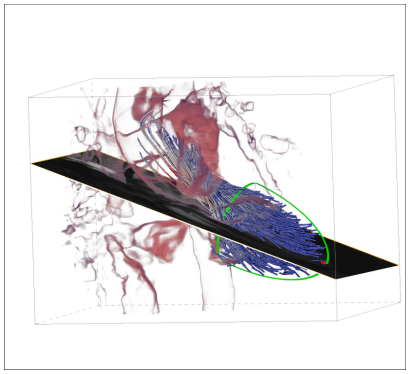

(c) Placement of the ellipsoid in the left ventricle. The pathlines show the blood flow from the LVE into the aorta at peak systole.

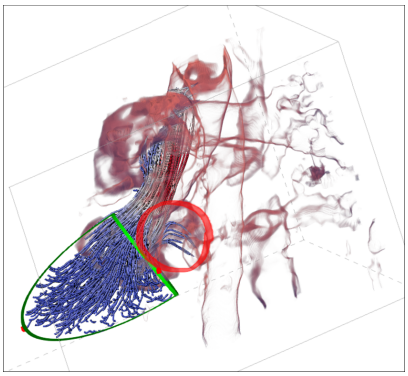

(d) Further expection shows blood flowing both in the aorta and the left atrium as indicated by the red circle. This suggests an aberrant flow pattern.

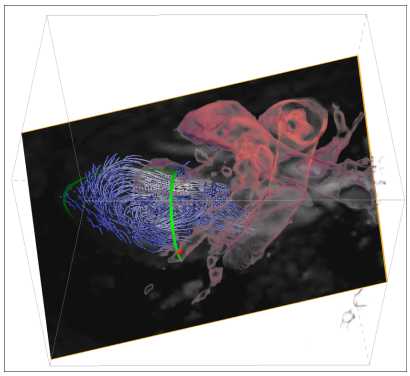

(e) Backward tracing pathlines from the left ventricle helps the alignment of a slice with the incoming flow.

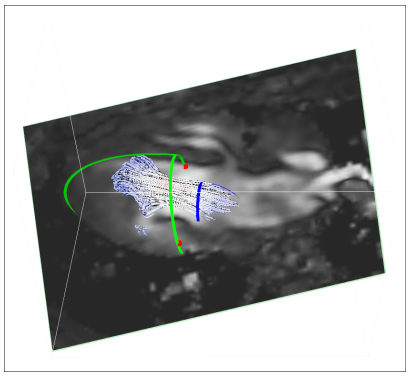

(f) Placement of a second ellipsoid, corresponding with the mitral valve. Flow is shown with forward tracing pathlines.

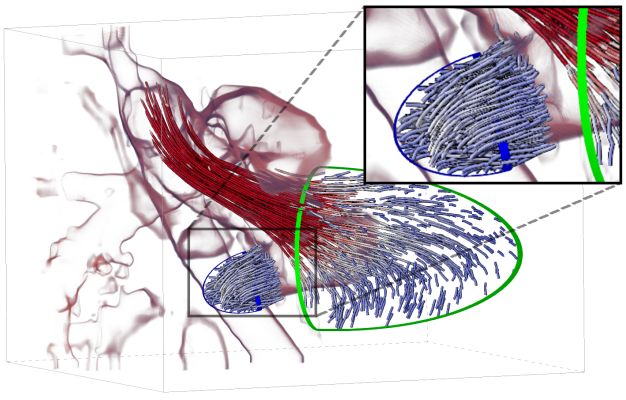

(g) Flow during peak systole in a healthy volunteer. The mitral valve prevents the flow from the left ventricle into the left atrium.

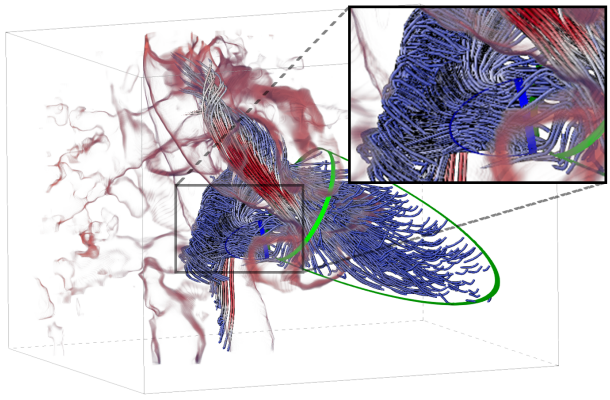

(h) Flow during peak systole in a patient. Blood flows to both the left atrium and left ventricle.

Figure 10: Steps followed in the use case. The coloring of the pathlines indicates speed: from blue (slow) to white to red (fast).

Statement	R1	R2	R3	R4	R5	R6	Agreement
The general structure of the heart can be perceived from the context	4	4	4	5	4	4	+
The context visualization helps with understanding the flow	2	4	5	4	5	4	+/-
The slices complement the volume rendering	3	5	4	4	5	4	+
The left ventricle can be approximated by LVE	5	4	4	4	4	4	+
The right ventricle can be approximated by RVE \ LVE	4	4	4	3	3	4	+
The placement and interaction with the ventricle ellipsoids is intuitive	5	4	4	4	4	4	+
Using an ellipsoid for clipping (compared to clipping planes) is suitable for heart data	4	4	4	4	3	4	+
Automatic seeding in areas of interest can be done based on flow features	5	5	4	4	4	4	+
Transfer functions are an intuitive way of specifying the properties of areas of interest	3	4	3	4	4	4	+/-
The project enables exploration, providing an overview of cardiac flow before using other methods for closer inspection	4	5	4	5	4	4	+

Table 1: Statements on the framework presented to 6 domain experts and their agreement with the statements.

structure of the vessels remains visible while obstructed view on the flow inside is minimized. Different lit sphere maps allowed for easy switching between different styles of visualization for the context. To improve depth perception, depth-based tone manipulation and depth-based transparency manipulation work well encoding the depth, improving the context visualization. The direct volume rendering of the t-MIP data provides no information about the current phase of the heart cycle, nor a clear distinction of the ventricles and atria. This is evaded by a slice-based visualizations by means of a multiplanar reformat and a view-orthogonal plane, on which the magnitude and velocity data can be shown.

The ventricles can be approximated by half-ellipsoids. Our ventricle ellipsoids definition use an intuitive method of interaction and can easily be placed. While the ventricle ellipsoids, as their name suggests, are intended for approximating the ventricles, they are not limited to that purpose. This was clearly demonstrated in the use case presented in this work, where one was placed behind the mitral valve to investigate its deficiency. For the clipping of data or the visualization, usually done using clipping planes, the half-ellipsoid proved to work well, since it fits the shape of the heart and structures within it much better, further enhancing the context visualization.

To aid in identifying interesting areas for flow inspection, and to automate seed point placement within such areas, feature-based seeding was implemented. Different features determining the area of interest can be chosen. The corresponding transfer functions made for an interactive method to define the interesting ranges of values. Using feature-based seeding, one can quickly identify regions with, for example, high speed vortices. The probability-based design allows to easily scale up to combinations of different features.

There are several points in which the framework could be extended. For example, the context visualization could be improved such that the ventricles and atria can be shown. If no additional imaging is desired, this would require a filtering and segmentation of the existsing data. Using the half-ellipsoids helps to provide a context for the flow visualization. However, these remain static over time, while the anatomy of the heart changes, rendering the approximation less suitable. Furthermore, using the half-ellipsoids does not aid to distinguish the atria and the ventricles clearly.

The ventricle ellipsoids can be used for other purposes as well. One could trace particles placed inside the ventricle, perform both backward and forward tracing and then classify them based on the resulting positions [CdKB*15]. This would provide additional information such as whether a particle enters the ventricle and leaves within one cycle or whether it stayed within the ventricle throughout the heart cycle.

The flow visualizations and seed placement provided could also be improved upon to avoid cluttering using for example techniques like hierarchical clustering of the flow [vPJtHRV12], dashtubes [FG98], or a combination with image-based seeding [LLS07].

A more thorough user study including more then 6 specialists would be beneficial. Such an user study should include tasks for the users to perform using the framework. Timing of these tasks then provides insight the learning curve of the framework.

Despite its limitations, the proposed framework allows researchers to explore the flow data without time consuming preprocessing and get a first insight on the obtained data.

References

[BCP*12] BRAMBILLA A., CARNECKY R., PEIKERT R., VIOLA I., HAUSER H.: Illustrative flow visualization: State of the art, trends and challenges. In *Eurographics 2012 - State of the Art Reports* (2012), The Eurographics Association. doi:10.2312/conf/EG2012/stars/075-094. 2

[BG07] BRUCKNER S., GRÖLLER M.: Style transfer functions for illustrative volume rendering. *Computer Graphics Forum 26*, 3 (2007), 715–724. 2, 3, 4

[CdKB*15] CALKOEN E., DE KONING P., BLOM N., KROFT L., DE ROOS A., WOLTERBEEK R., ROEST A., WESTENBERG J.: Disturbed intracardiac flow organization after atrioventricular septal defect correction as assessed with 4D flow magnetic resonance imaging and quantitative particle tracing. *Investigative radiology 50*, 12 (2015), 850–857. doi:10.1097/RLI.0000000000000194. 9

[CNC*10] COUSTY J., NAJMAN L., COUPRIE M., CL'EMENT-GUINAUDEAU S., GOISSEN T., GAROT J.: Segmentation of 4D cardiac MRI: Automated method based on spatio-temporal watershed cuts. *Image and Vision Computing 28*, 8 (2010), 1229–1243. doi:10.1016/j.imavis.2010.01.001. 2

[CNN*08] COCOSCO C., NIESSEN W., NETSCH T., VONKEN E., LUND G., STORK A., VIERGEVER M.: Automatic image-driven segmentation of the ventricles in cardiac cine MRI. *Journal of magnetic resonance imaging : JMRI 28*, 2 (2008), 366–374. doi:10.1002/jmri.21451. 2

[DGH03] DOLEISCH H., GASSER M., HAUSER H.: Interactive feature specification for focus+context visualization of complex simulation data. In *Proceedings of the Symposium on Data Visualisation 2003* (2003), pp. 239–248. 2

[EvdGC*16] ELBAZ M., VAN DER GEEST R., CALKOEN E., DE A. ROOS, LELIEVELDT B., ROEST A., WESTENBERG J.: Assessment of viscous energy loss and the association with three-dimensional vortex ring formation in left ventricular inflow: In vivo evaluation using four-dimensional flow MRI. *Magnetic Resonance in Medicine* (2016). doi:10.1002/mrm.26129. 1

[FG98] FUHRMANN A., GRÖLLER E.: Real-time techniques for 3D flow visualization. In *Proceedings of the conference on Visualization'98* (1998), pp. 305–312. doi:10.1109/VISUAL.1998.745317. 9

[GGSC98] GOOCH A., GOOCH B., SHIRLEY P., COHEN E.: A non-photorealistic lighting model for automatic technical illustration. In *Proceedings of the 25th annual conference on Computer graphics and interactive techniques* (1998), ACM, pp. 447–452. 4

[GNBP11] GASTEIGER R., NEUGEBAUER M., BEUING O., PREIM B.: The flowlens: A focus-and-context visualization approach for exploration of blood flow in cerebral aneurysms. *IEEE Transactions on Visualization and Computer Graphics 17*, 12 (2011), 2183–2192. doi:10.1109/TVCG.2011.243. 2

[GZM97] GUTTMAN M., ZERHOUNI E., MCVEIGH E.: Analysis of cardiac function from MR images. *IEEE computer graphics and applications 17*, 1 (1997), 30–38. doi:10.1109/38.576854. 2

[Hal05] HALLER G.: An objective definition of a vortex. *Journal of Fluid Mechanics 525* (2005), 1–26. doi:10.1017/S0022112004002526. 2

[HBB*10] HIRATZKA L., BAKRIS G., BECKMAN J., BERSIN R., CARR V., CASEY JR D., EAGLE K., HERMANN L., ISSELBACHER E., KAZEROONI E., KOUCHOUKOS N., LYTLE B., MILEWICZ D., REICH D., SEN S., SHINN J., SVENSSON L., WILLIAMS D.: Guidelines for the diagnosis and management of patients with thoracic aortic disease. *Journal of the American College of Cardiology 55*, 14 (Feb 2010), e27–e129. doi:10.1016/j.jacc.2010.02.015. 1

[HGL*14] HU H., GAO Z., LIU L., LIU H., GAO J., XU S., LI W., HUANG L.: Automatic segmentation of the left ventricle in cardiac MRI using local binary fitting model and dynamic programming techniques. *PLoS ONE 9*, 12 (2014), 1–17. doi:10.1371/journal.pone.0114760. 2

[JH95] JEONG J., HUSSAIN F.: On the identification of a vortex. *Journal of Fluid Mechanics 285* (1995), 69–94. doi:10.1017/S0022112095000462. 2

[KBKG07] KOHLMANN P., BRUCKNER S., KANITSAR A., GRÖLLER M.: Livesync: Deformed viewing spheres for knowledge-based navigation. *IEEE Transactions on Visualization and Computer Graphics 13*, 6 (2007), 1544–1551. 2

[KBvP*16] KÖHLER B., BORN S., VAN PELT R., HENNEMUTH A., PREIM U., PREIM B.: A survey of cardiac 4d pc-mri data processing. *Computer Graphics Forum* (2016). URL: http://dx.doi.org/10.1111/cgf.12803, doi:10.1111/cgf.12803. 2

[KNC*05] KOVALOVA S., NECAS J., CERBAK R., MALIK P., VESPALEC J.: Echocardiographic volumetry of the right ventricle. *European journal of echocardiography 6*, 1 (2005), 15–23. doi:10.1016/j.euje.2004.04.009. 2, 5

[KWTM03] KINDLMANN G., WHITAKER R., TASDIZEN T., MOLLER T.: Curvature-based transfer functions for direct volume rendering: Methods and applications. In *Proceedings of the 14th IEEE Visualization 2003* (2003), IEEE Computer Society. doi:10.1109/VISUAL.2003.1250414. 2, 3

[LGW06] LYNCH M., GHITA O., WHELAN P.: Automatic segmentation of the left ventricle cavity and myocardium in MRI data. *Computers in Biology and Medicine 36*, 4 (2006), 389–407. doi:10.1016/j.compbiomed.2005.01.005. 2

[LLS07] L. LI L., SHEN H.: Image-based streamline generation and rendering. *IEEE Transactions on Visualization and Computer Graphics*, 3 (2007), 630–640. doi:10.1109/TVCG.2007.1009. 9

[LM02] LUM E., MA K.: Hardware-accelerated parallel non-photorealistic volume rendering. In *Proceedings of the 2nd international symposium on Non-photorealistic animation and rendering* (2002), ACM. 4

[Mea15] MOZAFFARIAN D., ET AL.: Heart disease and stroke statistics–2015 update: a report from the American Heart Association. *Circulation 131*, 4 (Jan 2015), e29–e322. 1

[MFK*12] MARKL M., FRYDRYCHOWICZ A., KOZERKE S., HOPE M., WIEBEN O.: 4D flow MRI. *Journal of Magnetic Resonance Imaging 36*, 5 (2012), 1015–1036. doi:10.1002/jmri.23632. 1, 2

[MM09] MUELDER C., MA K. L.: Interactive feature extraction and tracking by utilizing region coherency. In *2009 IEEE Pacific Visualization Symposium* (2009), pp. 17–24. doi:10.1109/PACIFICVIS.2009.4906833. 2

[PVH*03] POST F., VROLIJK B., HAUSER H., LARAMEE R., DOLEISCH H.: The state of the art in flow visualisation: Feature extraction and tracking. *Computer Graphics Forum 22*, 4 (2003), 775–792. doi:10.1111/j.1467-8659.2003.00723.x. 2

[SAG*14] STANKOVIC Z., ALLEN B., GARCIA J., JARVIS K., MARKL M.: 4D flow imaging with MRI. *Cardiovascular diagnosis and therapy 4*, 2 (2014), 173–192. doi:10.3978/j.issn.2223-3652.2014.01.02. 2

[SMGG01] SLOAN P., MARTIN W., GOOCH A., GOOCH B.: The lit sphere: A model for capturing npr shading from art. In *Proceedings of the Graphics Interface 2001 Conference, June 7-9 2001, Ottawa, Ontario, Canada* (2001), pp. 143–150. 2, 4

[SV97] SÖRGEL W., VAERMAN V.: Automatic heart localization from a 4D MRI dataset. In *In Proc. of the SPIE Conference on Medical Imaging* (1997), pp. 333–344. 2

[SZH97] STALLING D., ZOCKLER M., HEGE H.: Fast display of illuminated field lines. *IEEE Transactions on Visualization and Computer Graphics 3*, 2 (1997), 118–128. doi:10.1109/2945.597795. 2, 6

[vPBB*10] VAN PELT R., BESCOS J. O., BREEUWER M., CLOUGH R. E., GRÖLLER M. E., TER HAAR ROMENIJ B., VILANOVA A.: Exploration of 4D MRI blood flow using stylistic visualization. *IEEE Transactions on Visualization and Computer Graphics 16*, 6 (2010), 1339–1347. doi:10.1109/TVCG.2010.153. 2, 3

[vPBB*11] VAN PELT R., BESCOS J. O., BREEUWER M., CLOUGH R., GRÖLLER M., TER HAAR ROMENIJ B., VILANOVA A.: Interactive virtual probing of 4D MRI blood-flow. *IEEE Transactions on Visualization and Computer Graphics 17*, 12 (2011), 2153–2162. doi:10.1109/TVCG.2011.215. 2

[vPFCV14] VAN PELT R., FUSTER A., CLAASSEN G., VILANOVA A.: Characterization of blood-flow patterns from phase-contrast MRI velocity fields. In *EuroVis - Short Papers* (2014). doi:10.2312/eurovisshort.20141158. 2

[vPJtHRV12] VAN PELT R., JACOBS S., TER HAAR ROMENY B., VILANOVA A.: Visualization of 4D blood-flow fields by spatiotemporal hierarchical clustering. In *Computer Graphics Forum* (2012), vol. 31, pp. 1065–1074. doi:10.1111/j.1467-8659.2012.03099.x. 9

[WEE02] WEISKOPF D., ENGEL K., ERTL T.: Volume clipping via per-fragment operations in texture-based volume visualization. In *Proceedings of the Conference on Visualization '02* (2002), IEEE Computer Society, pp. 93–100. 2

[YPH*06] YUSHKEVICH P., PIVEN J., HAZLETT H., SMITH R., HO S., GEE J., GERIG G.: User-guided 3D active contour segmentation of anatomical structures: Significantly improved efficiency and reliability. *NeuroImage 31*, 3 (2006), 1116–1128. doi:10.1016/j.neuroimage.2006.01.015. 2